Phylogeography of Fungicide Resistance of *Alternaria alternata* and *Alternaria tenuissima* to Demethylation Inhibitor Fungicides

Robbi Miguel G. Falcon*
College of Medicine
University of the Philippines Manila

Leilani G. Sumabat-Dacones
Institute of Biology
University of the Philippines Diliman

ABSTRACT

Demethylation inhibitors (DMI) fungicides are commonly used to mitigate fungal diseases in crops by inhibiting ergosterol biosynthesis. *Alternaria alternata* and *Alternaria tenuissima* are fungal plant pathogens being controlled with DMIs. However, with unregulated use of fungicides, reports on reduced sensitivity to DMIs have been documented in these fungal species. Previous studies have shown the accumulation of point mutations in *CYP*51 and *CYP*61 genes that are involved in ergosterol biosynthesis to the development of resistance to DMI fungicides. Understanding the phylogeographic trends of isolates based on the DMI gene targets is critical to identify sustainable management strategies against fungicide resistance. In this study, a phylogenetic approach was used to determine the association of geographic origin of isolates with fungicide resistance across *A. alternata* and *A. tenuissima* isolates. Phylogeographic and haplotype analyses revealed genetic patterns in *CYP*51 and *CYP*61, associated with DMI resistance. Generally, clusters formed within specific geographic areas such as Asia and North America. Moreover, nucleotide variation estimates revealed the presence of polymorphic nucleotide bases in response to DMI exposure as a selection pressure. These results provided insights in further testing in vitro assays regarding the selection patterns associated with specific regions.

Keywords: Alternaria leaf spot, nucleotide variations, ergosterol biosynthesis, *CYP51*, triazole fungicides

* *Corresponding Author*

INTRODUCTION

Fungal plant pathogens are often regarded as one of the leading determinants in the agricultural industry of the Philippines. *Alternaria* sp. is an example of a prevalent type of fungal pathogen across the world (Malandrakis et al. 2015; Avenot et al. 2016; He et al. 2019). Species of widespread pathogenic *Alternaria* spp., such as the *Alternaria alternata* and *Alternaria tenuissima*, are known to target agriculturally significant produce such as tomatoes and small-grain cereals (Pastor and Guarro 2008; Ozkilinc and Kurt 2017). Generally, these two species of fungal pathogens are known to exhibit similar genetic characteristics and are taxonomically distinguished from each other based on morphology (Rajarammohan et al. 2019). Studies show that many regions across the world have been struck with postharvest decay due to Alternaria leaf spot infections (Patriarca and Fernández Pinto 2018).

In agriculture, the use of fungicides is a common practice against rapidly populating fungal pathogens. One class of commonly used fungicides are the demethylation inhibitor (DMI) fungicides. DMI fungicides inhibit the activity of essential biotransformation enzymes known as cytochrome P450 monooxygenases (*CYP*), which are involved in the biosynthesis of ergosterol (Loto et al. 2012; He et al. 2019). One of the most common groups of DMI fungicides used in agriculture are triazoles, which inhibit the synthesis of sterol, an essential structural and functional component of the fungal cell membrane (He et al. 2019; Gai et al. 2021). One commonly known inhibition target in the mechanism of ergosterol biosynthesis is the conversion of lanosterol to ergosterol (Shalini et al. 2011). Sterol synthesis is mediated by enzymes coded by genes such as *CYP*51 and *CYP*61, which are highly conserved across most fungi and consequently the primary targets of triazoles (Loto et al. 2012). However, due to the specificity of triazole action, fungal pathogens are known to frequently develop resistance by genetic modification (Zeiner et al. 2016; Zhang et al. 2019). Moreover, unregulated usage of specific action fungicides has also contributed to the development of resistance.

Recent advancements in genetic studies show that the development of fungicide resistance is primarily attributed to adaptive changes at the molecular level. These range from point mutations, genomic plasticity, upregulation of transcription factors, and several underlying mutative responses (Deising et al. 2008). Adaptive mechanisms responsible for the development of fungicide resistance typically vary based on the geographic location of the fungal pathogen, the frequency of fungicidal exposure, and susceptibility to mutations (Chen et al. 2014; He et al. 2019). Such variations arise due to responses across populations, causing resistant mutants

to persist and populate. However, these genetic changes lead to severe fitness penalties, resulting in several structural and functional changes across resistant mutants (Zhang et al. 2019; Zhang et al. 2020). The usage of dynamic management programs based on the underlying principles of the development of resistance in populations has become more prominent in the control of fungal pathogens (He et al. 2019). Typically, the effective concentration (EC_{50}) value is used to determine the resistance of a fungal pathogen to a specific fungicide. This corresponds to the minimum concentration of fungicide needed to elicit a response halfway through the maximal and baseline effect (Rosenzweig et al. 2019; Yang et al. 2019). The EC_{50} parameter is commonly used in vitro to determine the sensitivity patterns of fungal pathogens to specific fungicides. Integration of factors, such as sensitivity patterns, geographic location, host species of origin, and the phylogenetic history of populations of *A. alternata* and *A. tenuissima*, is vital for the development of effective preventive measures (He et al. 2019; Zhang et al. 2019; Zhang et al. 2020). Therefore, phylogeographic studies are needed to further elaborate the fungicidal mechanisms utilized by such fungal pathogens.

This study primarily aims to determine the phylogeography of fungicide resistance of *Alternaria alternata* and *A. tenuissima* to DMI fungicides by comparing nucleotide sequence and EC_{50} data. It is hypothesized that DMI fungicide resistance of *A. alternata* and *A. tenuissima* are widely distributed and phylogenetically distinct across geographic locations and host species of origin.

In this study, genome sequences of isolates both with known and undetermined sensitivity to DMI fungicides acquired from open-access databases were compared for genetic variations. Moreover, phenotypic characteristics, represented by the sensitivity profiles of the isolates, were used to elucidate the underlying mechanism and relationship of factors involved in the development of DMI fungicide resistance in *A. alternata* and *A. tenuissima*. To address these objectives, first, the prevalence of fungicide resistance of *A. alternata* and *A. tenuissima* to commonly used DMI fungicides across geographic location and host species of origin was determined. Second, the phylogenetic relationships of *A. alternata* and *A. tenuissima* across geographic location and host species of origin based on *CYP*51 and other related gene targets of DMI fungicides were identified. Last, the genetic clustering patterns and population structure of *A. alternata* and *A. tenuissima* were determined. From the result of these activities, the evolutionary mechanisms of fungicide resistance mechanisms were established. The findings of the study allowed for the development of sustainable mitigation methods against the spread of fungal diseases in the agricultural industry.

MATERIALS AND METHODS

Survey on genetic patterns of *A. alternata* and *A. tenuissima* isolates in relation to geographical and host species of origin. Documented cases of fungicide resistance of *A. alternata* to DMI fungicides were compiled, including those from plant disease notes, nucleotide/amino acid sequence submissions, and other open-access databases (i.e., FungiDB, NCBI Genbank, JGI-DOE, and the European Nucleotide Archive). A total of 15 whole genome assemblies of *A. alternata*, eight whole genome assemblies of *A. tenuissima*, and 1 *CYP*51 gene region of *A. alternata* isolates were retrieved. The number of sequences included in the phylogenetic analysis was limited to the curated data available from the open-access databases surveyed. Genetic, geographical, and host species patterns were surveyed from the corresponding literature publications and other sources of metadata for each nucleotide sequence used and tabulated for each species (Table 1). The nucleotide sequences of *CYP*51, *CYP*61, and ITS regions from *A. alternata* and *A. tenuissima* were obtained and consolidated into corresponding sequence alignment files to be analyzed for geographic and genetic relationships. For the *A. alternata* Hei146 isolate, only the *CYP*51 gene region was available, with the *CYP*61 and ITS gene regions not found in NCBI GenBank. Corresponding gene regions and other genetic patterns from the whole genome assemblies were datamined using BLAST with the annotated reference genomes of *A. alternata* (GCF_001642055.1) and *A. tenuissima* (GCA_004156035.1) from NCBI Genbank. Other notable molecular patterns in the nucleotide sequences from gene regions obtained from whole genome assemblies of *A. alternata* and *A. tenuissima*, together with available metadata, were surveyed and noted for further analysis. Certain sequence datasets were curated without complete metadata or sensitivity profiles, thus serving as a major limitation of the study. Moreover, certain geographic regions also currently do not have any reported sequence datasets of *A. tenuissima*, limiting the scope of the current study.

Mean EC_{50} value comparisons of ***A. alternata*** tested with commonly used DMI fungicides. EC_{50} values of three commonly used DMI fungicides - difenoconazole, tebuconazole, and propiconazole – from various studies on *A. alternata* populations across different geographical regions and host species of origin were gathered. From the studies, information on the year of sample collection, number of isolates collected, host species of origin, and the geographic location was compiled and tabulated (Table 2). Box plot representations were generated to illustrate the statistical trends of the EC_{50} values. The mean, maximal, and minimum values were indicated in the box plot. The reported EC_{50} served as a replicate for the mean

comparisons analysis to determine the phenotypic pattern of fungicide resistance (Table 3). Mean EC_{50} values for each data sets were tested for statistical significance using one-way ANOVA at $\alpha \leq 0.05$ on SPSS (version 20) (Ostertagova et al. 2013).

Table 1. Origin of *A. alternata* and outgroup ergosterol-related gene sequences across geographic location and host species of origin

Isolate Name	Accession Number	Citation	Host	Location
		(A) *A. alternata*		
FERA 1177	GCA_004154755.1	(Armitage et al. 2020)	Malus domestica	UK
MPI-PUGE-AT-0064	N/A[1]	(Mesny et al. 2021)	Arabidopsis thaliana	Germany
B2a	GCA_001696825.1	(Bihon et al. 2016)	*Allium cepa*	South Africa
SRC1lrK2f	GCF_001642055.1	(Zeiner et al. 2016)	N/A[3]	USA
ATCC 11680	N/A[1]	(Dang et al. 2015)	N/A[2]	USA
ATCC 66891	N/A[1]	(Dang et al. 2015)	N/A[2]	USA
ATCC 34957[s]	GCA001443195.1	(Nguyen et al. 2016)	*Sorghum bicolor*	Canada
BMP 0270	N/A[1]	(Dang et al. 2015)	N/A[2]	USA
MOD1-FUNG5	GCA_004634295.1	(Gebru et al. 2020)	*Vitis labrusca*	USA
Hei146[s]	MN542657	(Zhang et al. 2020)	*Coleus rotundifolius*	China
Z7	GCA_001572055.1	(Gai et al. 2019)	*Citrus reticulata*	China
NAP07	GCA_009932595.1	(Gai et al. 2019)	*Prunus persica*	Japan
EV-MIL-31	GCA_016097525.1	(Wu et al. 2023)	*Citrus suavissima*	Taiwan
PN1	GCA_011420445.1	(Rajarammohan et al. 2019)	*Brassica juncea*	India
PN2	GCA_011420565.1	(Rajarammohan et al. 2019)	*Brassica juncea*	India
JS-1623	GCA_009650635.1	(Park et al. 2020)	*Abies koreana*	Korea
P-A14[4]	GCA_014334815.1	(Tamang et al. 2019)	*Hordeum vulgare*	USA
		(B) *A. tenuissima*		
FERA 635	GCA_004168565.1	(Armitage et al. 2020)	*Malus domestica*	United Kingdom
FERA 648	GCA_004154765.1	(Armitage et al. 2020)	*Malus domestica*	United Kingdom
FERA 743	GCA_004154845.1	(Armitage et al. 2020)	*Malus domestica*	United Kingdom
FERA 1082	GCA_004154745.1	(Armitage et al. 2020)	*Malus domestica*	United Kingdom
FERA 1164	GCA_004156015.1	(Armitage et al. 2020)	*Malus domestica*	United Kingdom
FERA 1166	GCA_004156035.1	(Armitage et al. 2020)	*Malus domestica*	United Kingdom
FERA 24350	GCA_004154735.1	(Armitage et al. 2020)	*Malus domestica*	United Kingdom
BMP 0304[s]	N/A[1]	(Dang et al. 2015)	N/A[2]	USA

[s]Refers to sensitive Alternaria alternata and A. tenuissima isolates used as standards for the analysis. [1]Sequence data was obtained from JGI-DOE Mycocosm. [2]Host species of origin of isolate was not indicated in original publication; [3]Isolate was obtained from passive coal mine drainage treatment systems; [4]The designated outgroup, Pyrenophora teres f. maculate,

where phylogenetic tree was rooted.

Table 2. Mean effective concentrations (EC_{50}) values for isolates of *A. alternata* across various geographic locations and host species of origin tested with commonly used DMI fungicides - difenoconazole, tebuconazole, and propiconazole

Fungicide	Citation	Number of Isolates	Year of Collection	Host Species of Origin	Location	EC_{50} (µg/mL)
Difenoconazole	(Avenot et al. 2016)	65	2012	Pistacia vera	USA	0.06
Difenoconazole	(Amrate et al. 2013)	3	2012	Aloe barbadensis	India	1.70
Difenoconazole	(Fu et al. 2017)	54	2012	*Citrus reticulata*	China	0.61
Difenoconazole	(Zhang et al. 2020)	160	2019	*Coleus rotundifolius*	China	1.68
Tebuconazole	(Avenot et al. 2016)	65	2012	*Pistacia vera*	USA	0.51
Tebuconazole	(Amrate et al. 2013)	3	2012	*Aloe barbadensis*	India	3.30
Tebuconazole	(Fu et al. 2017)	54	2012	*Citrus reticulata*	China	0.56
Tebuconazole	(Ali et al. 2019)	3	2017	*Triticum aestivum*	Egypt	1.70
Propiconazole	(Avenot et al. 2016)	46	2003	*Pistacia vera*	USA	1.29
Propiconazole	(Avenot et al. 2016)	38	2010	*Pistacia vera*	USA	1.25
Propiconazole	(Amrate et al. 2013)	3	2012	*Aloe barbadensis*	India	5.80
Propiconazole	(Ozkilinc and Kurt 2017)	22	2016	*Pistacia* sp.	Turkey	0.01

Table 3. Mean, standard deviation, and standard error of EC_{50} values (µg/mL) for isolates of *A. alternata* across different types of DMI fungicides

Type of Fungicide[1]	N[2]	Mean[3]	SD[4]	SE[5]
Difenoconazole	4	1.0125	0.81394	0.40697
Tebuconazole	4	1.5175	1.30926	0.65463
Propiconazole	4	2.0875	2.54533	1.27266
Total	12	1.5392	1.62033	0.46775

[1]Type of DMI fungicide treatment tested in original publication; [2]Number of studies corresponding as replicates for treatments; [3]Mean EC_{50} value across replicates (µg/mL); [4]Standard deviation across replicates; [5]Standard error across replicates.

Generation of sequence alignment file. Whole genome assemblies of *A. alternata* and *A. tenuissima* were obtained from open-access databases. *CYP*51, *CYP*61, and ITS gene regions were compared using BLAST with annotated gene regions obtained from reference sequences. The designated gene regions were extracted and edited using BioEdit (version 7.2.5). Edited gene region sequences were then aligned and a PHYLIP sequence alignment file format was generated using Geneious Prime (Biomatters Ltd.) (version 2021.0.3) (Hall 2013).

Construction of NJ & ML phylogenetic trees. Phylogenetic trees of the *CYP*51 and *CYP*61 gene regions were constructed using the neighborhood-joining (NJ) method and maximum likelihood (ML) method for each of the *Alternaria* spp. The NJ method

was coded on PAUP* (version 4b10) based on HKY85 and TN93 models for DNA sequence evolution (Swofford 2003). The ML tree was generated using the program MEGA (version 10.2.4) based on the HKY85 and TN93 models for DNA sequence evolution (Hall 2013). The trees were rooted on the outgroup, *Pyrenophora teres* f. *maculata*, due to its genomic similarity and distinct phylogenetic relationship with the *Alternaria* spp. (Schoch et al. 2009). A statistical test for congruence between the NJ and ML trees was conducted using the non-parametric bootstrapping method with 500 replicates (Arnaoudova et al. 2010).

Construction of TCS haplotype networks. Haplotype networks based on the *CYP*51 and *CYP*61 nucleotide alignments of each of the *Alternaria* spp. were constructed using the program, TCS (version 1.23) under statistical parsimony (Snell et al. 2002). Generated haplotype networks were edited on tcsBU which were color-coded based on geographic region and patterned based on reported sensitivity patterns to DMI fungicides (dos Santos et al. 2016). The frequency of isolates of haplotypes for each gene is shown in Table 4.

Table 4. Haplotype frequency of isolates of *Alternaria alternata* and *A. tenuissima* based on *CYP*51 and *CYP*61 across geographic regions

Haplotype	Frequency	Isolates
(A) *Alternaria alternata* – *CYP*51		
Hap_A1	1	PN2
Hap_A2	9	ATCC 11680, BMP 0270, MOD1-FUNG5, Z7, NAP07, JS-1623, FERA 1177, MPI-PUGE-AT-0064, B2a
Hap_A3	1	EV-MIL-31
Hap_A4	2	SRC1lrK2f, ATCC 66891
Hap_A5	1	PN1
Hap_A6	1	ATCC 34957
Hap_A7	1	Hei146
(B) *Alternaria alternata* – *CYP*61		
Hap_B1	1	B2a
Hap_B2	1	FERA 1177
Hap_B3	1	ATCC 34957
Hap_B4	1	JS-1623
Hap_B5	1	Z7
Hap_B6	1	MPI-PUGE-AT-0064
Hap_B7	1	MOD1-FUNG5
Hap_B8	3	ATCC 66891, BMP 0270, PN1
Hap_B9	1	NAP07
Hap_B10	1	ATCC 11680
Hap_B11	2	SRC1lrK2f, PN2
Hap_B12	1	EV-MIL-31
(C) *Alternaria tenuissima* – *CYP*51		
Hap_C1	1	FERA 648
Hap_C2	5	FERA 635, FERA 743, FERA 1082, FERA 1166, BMP 0304
Hap_C3	2	FERA 1164, FERA 24350
(D) *Alternaria tenuissima* – *CYP*61		
Hap_D1	1	FERA 1166
Hap_D2	2	FERA 24350, BMP 0304
Hap_D3	4	FERA 635, FERA 743, FERA 1082, FERA 1164
Hap_D4	1	FERA 648

Estimation of genetic clustering patterns of populations of *A. alternata* and *A. tenuissima*. The nucleotide sequence data for both *CYP*51 and *CYP*61 used for both species in the phylogenetic analysis was concatenated with corresponding ITS regions on Geneious Prime (Biomatters Ltd.) (version 2021.0.3). The ITS regions were obtained from the NCBI Genbank and JGI-DOE database. The diversity parameters estimated in DnaSP (version 6.12.03) include the number of variable sites (VS), nucleotide diversity (π), haplotype diversity (Hd), the number of haplotypes, Tajima's D value, and Watterson's estimator (Θ_w) (Rozas et al. 2017). Inferences about the population structure and occurrence of selection were determined based on the genetic parameters estimated.

RESULTS

Survey on genetic, geographical, and host species patterns of *A. alternata* and *A. tenuissima* isolates. A survey of literature reports on nucleotide sequence data of *A. alternata* and *A. tenuissima CYP*51 and *CYP*61 gene regions was conducted. Results of the survey were tabulated based on geographic region and host species of origin. From the consolidated data, two reported sensitive isolates from North America (ATCC 34957) and China (Hei146) were identified based on the metadata gathered from the sequence dataset (Table 1). Pairwise alignments of the sequence data showed high sequence similarity across all isolates used based on BLAST identity. Numerous point mutations were observed across the nucleotide sequences of all isolates from both species. For *A. alternata* isolates, only one North American isolate (SRC1lrK2f) isolated from sewage treatment showed distinctive large gaps along the *CYP*51 gene region whereas single point mutations were observed in the corresponding *CYP*61 gene region of the isolate. In general, greater genetic variability was observed across *CYP*61 gene regions than in *CYP*51 gene regions of *A. alternata*. In contrast, both *CYP*51 and *CYP*61 gene regions of *A. tenuissima* exhibited a similar degree of genetic variation. As for *A. tenuissima* isolates, only two geographic regions were represented – Europe and North America. However, two European isolates of *A. tenuissima* (FERA 635 and FERA 1082) were shown to be completely identical in both gene regions. Genetic clustering patterns based on pairwise observations on the BLAST identity of nucleotide sequences of *CYP*51 and *CYP*61 gene regions from *A. alternata* and *A. tenuissima* showed high sequence similarity between both species.

Mean EC_{50} comparisons of *A. alternata* tested with commonly used DMI fungicides. Phenotypic characterization of the development of DMI fungicide resistance in *A. alternata*, was conducted by statistical analyses using the mean EC_{50} values

reported in studies across various geographic regions and host species of origin (Table 3). Based on the reported studies, one of the most abundant types of DMI fungicide currently being used are azoles – with difenoconazole, tebuconazole, and propiconazole being the most prominent. From these studies, the mean EC_{50} and corresponding standard deviation values for each dataset of *A. alternata* tested with difenoconazole (μ=1.01, SD=0.81), tebuconazole (μ=1.52, SD=1.31), and propiconazole (μ=2.09, SD=2.55) were analyzed with one-way ANOVA using SPSS (version 20). Previous studies suggest that isolates with EC_{50} values less than 0.1 μg/mL are classified as sensitive, followed by isolates with EC_{50} values between 0.1 μg/mL and 1 ug/mL are classified as tolerant, and isolates with EC_{50} values greater than 1 μg/mL are classified as resistant (Chong et al. 2021). From these threshold values, *A. alternata* samples from across the globe have exhibited significant levels of fungicide resistance across different geographic regions.

Levene's Test of Homogeneity of Variances revealed no significant difference between the group variances tested with difenoconazole, tebuconazole, and propiconazole. This would indicate no significant difference in the levels of fungicide resistance across the three types of DMI fungicides. Based on the generated box plots, the median line of each box for each dataset coincided along each interquartile range – reinforcing the findings of the statistical analyses. Furthermore, there was no significant difference between the group means of EC_{50} values across isolates tested with difenoconazole, tebuconazole, and propiconazole as determined by one-way ANOVA ($F(2,9) = 0.392$, $p = .687$).

Construction of NJ and ML phylogenetic trees. Phylogenetic trees for each gene generated by NJ and ML produced similar topologies with branch lengths representing the genetic distance of each isolate. Bootstrap replicates indicate a generally well-supported tree topology for each species based on both methods used. All nucleotide sequences used showed optimal E, percent identity, and query cover values. The sensitive *A. alternata* isolates, Hei146 and ATCC 34957, formed a well-supported distinct clade which clustered together with two North American (SRC1lrK2f & ATCC 66891) and two Asian (PN1 & EV-MIL-31) isolates based on the *CYP*51 gene region. This clustering pattern was well-supported by bootstrap values, indicating a high likelihood of genetic similarity between isolates found within this clade. Moreover, both the European and African isolates clustered with the remaining North American and Asian isolates, having identical genetic sequences. This represented the second genetically distinct group, indicating the presence of two distinct clades (Figure 1A). In contrast, the clusters formed based on the *CYP*61 gene varied significantly when compared to the *CYP*51 tree. The Asian isolate,

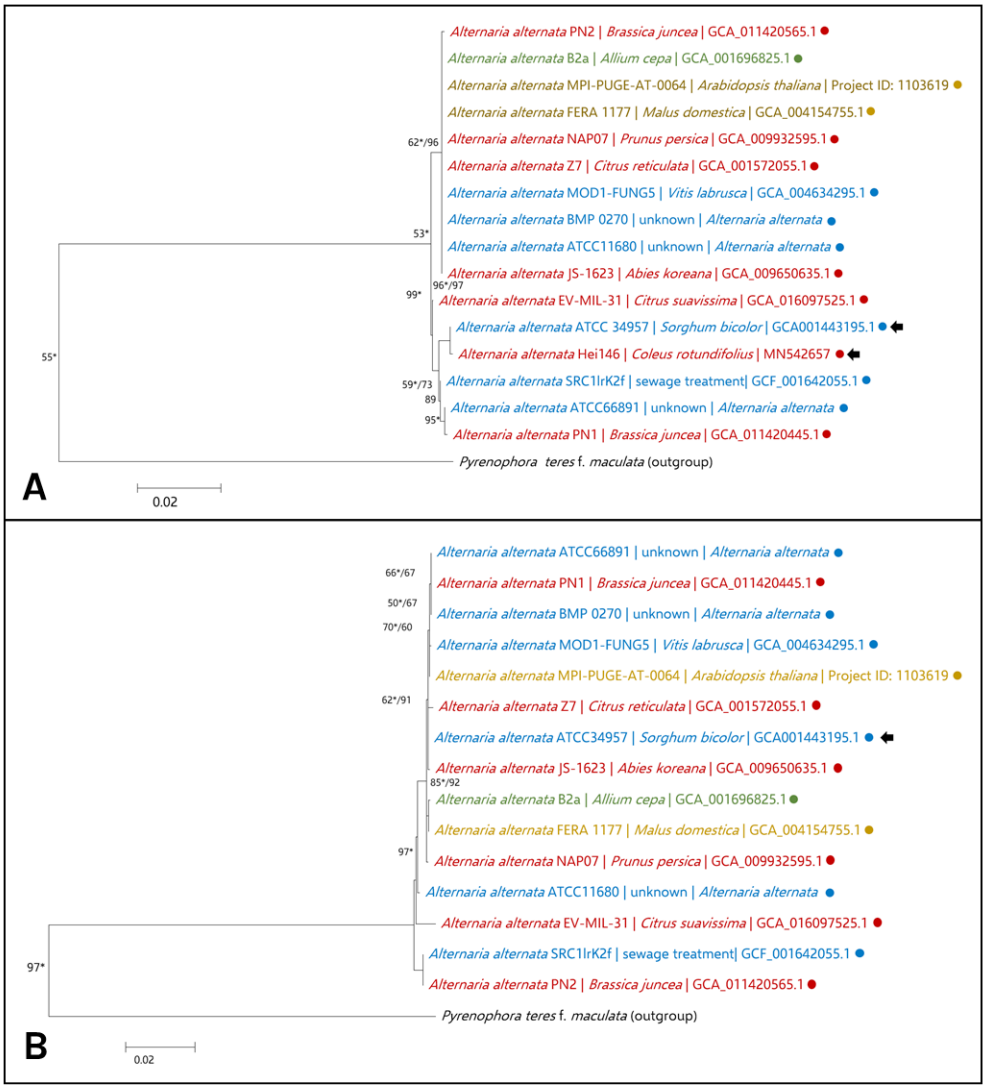

Figure 1. Maximum Likelihood Tree of (A) 16 isolates of *Alternaria alternata* (based on 1683 nucleotides of the *CYP*51 gene) using the HKY85 model and (B) 15 isolates of *Alternaria alternata* (based on 2190 nucleotides of the *CYP*61 gene) using the TN93 model. The tree is rooted on *Pyrenophora teres* f. *maculata*, values on nodes represent percentage bootstrap support out of 500 bootstrap samples; bootstrap values less than 50% are NOT shown. Branch terminals were labeled based on host species/origin of isolate (if environmental sample) and accession number. Bootstrap support values marked with an asterisk (*) were generated using PAUP* (version 3b10) while unmarked values were generated using MEGA (version 10.2.5) (Swofford 2003; Kumar et al. 2018). Scale bar represents 2 nucleotide substitutions for every 100 nucleotides. Each isolate was color-coded based on geographic region (Asia – red, Africa – green, Europe – yellow, North America – blue). The sensitive isolates are denoted with a black arrow.

JS-1623, was found closest to the sensitive isolate, ATCC 34957. The SRC1lrK2f isolate clustered separately from ATCC 66981, which was found with PN1, and was instead found with the Asian isolate, PN2. Asian isolate, EV-MIL-31, formed its own distinct group, branching from other clades. Overall, no distinctive pattern of clustering was observed in the *CYP*61 phylogenetic tree for *A. alternata* (Figure 1B). For *A. tenuissima*, two distinct clades formed in the phylogenetic trees for *CYP*51. In the CYP61 phylogenetic tree, the sensitive North American isolate BMP 0304, possessed an identical genetic code and clustered together with all other European isolates, except for isolates FERA 1164 and FERA 24350 which had formed a separate group (Figure 2A). In contrast, the BMP 0304 isolate, designated as the sensitive isolate, was observed clustering with the FERA 24350 isolate based on the *CYP*61 gene region. Moreover, the FERA 1166 was distinct and formed its own lineage separate from the clade formed by the other European isolates and North American isolates (Figure 2B). In summary, the phylogenetic patterns observed indicated high sequence similarity in the *CYP*51 gene region of sensitive *A. alternaria* isolates, with no distinctive clustering pattern being present in the *CYP*61 gene region phylogeny. This pattern was not clearly observable in across *A. tenuissima* isolates, for both gene regions.

Construction of TCS haplotype networks. The haplotype networks constructed for each gene showed similar topologies to the corresponding phylogenetic trees generated. Color-coded circles represent each individual isolate with white circles indicating the number of putative sites corresponding to mutation events between each isolate. The sizes of the colored circles indicated the number of isolates found within the haplotype. Based on the *CYP*51 gene, 9 *A. alternata* isolates are generally clustered together to form the haplotype, HAP_A2 (Table 4). The Asian isolate, PN2, formed its own distinct isolate mutating at one site compared to isolates of HAP_A2. All other haplotypes appeared to arise from a similar lineage to that of the HAP_A6 and HAP_A7 containing sensitive isolates, ATCC 34957 and Hei146. Only HAP_A5, containing the isolate PN1, appeared to branch separately from HAP_A4 (Figure 3A). For the haplotype network generated for the *CYP*61, haplotypes branched from the haplotype HAP_B3 containing the sensitive isolate ATCC 34957, form four distinct lineages. The closest haplotype, HAP_B4, contained the isolate JS-1623. The haplotype HAP_B5, containing the isolate Z7, formed a relatively closely related lineage to the sensitive isolate. Haplotypes HAP_B6, HAP_B7, and HAP_B8 formed a distinct lineage, with isolates of HAP_B7 and HAP_B8 branching from the European isolate, MPI-PUGE-AT-0064. The fourth lineage from HAP_B3 branched into three, two of which correspond to the lineage of HAP_B9 and the lineage of HAP_B2 and HAP_B1. The third lineage consisted of haplotypes, HAP_B10, HAP_B11,

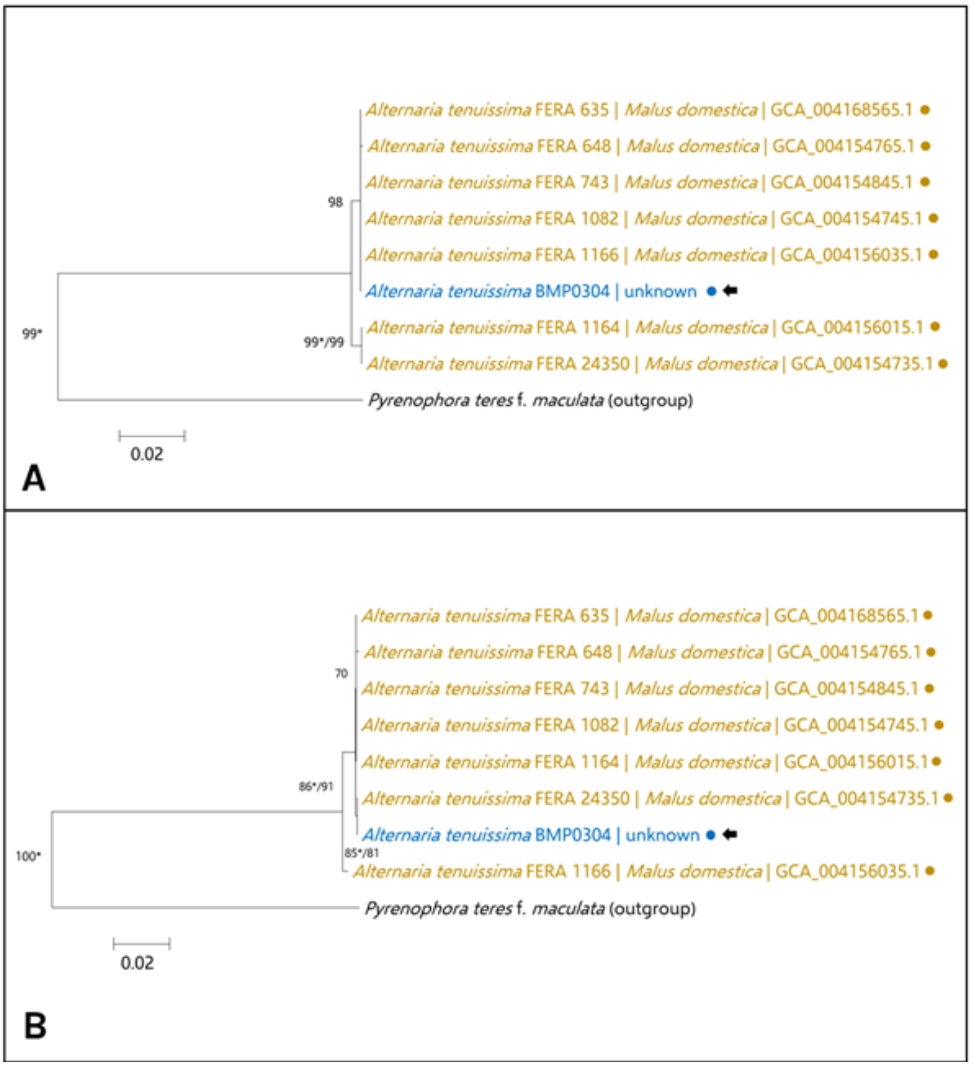

Figure 2. Maximum Likelihood Tree of (A) 8 isolates of *Alternaria tenuissima* based on 1682 nucleotides of the *CYP*51 gene using the HKY85 model and (B) on 2213 nucleotides of the *CYP*61 gene using the TN93 model. The tree is rooted on *Pyrenophora teres* f. *maculata*, values on nodes represent percentage bootstrap support out of 500 bootstrap samples; bootstrap values less than 50% are NOT shown. Branch terminals were labeled based on host species/ origin of isolate and accession number. Bootstrap support values marked with an asterisk (*) were generated using PAUP* (version 3b10) while unmarked values were generated using MEGA (version 10.2.5) (Swofford 2003; Kumar et al. 2018). Scale bar represents 2 nucleotide substitutions for every 100 nucleotides. Each isolate was color-coded based on geographic region (Asia – red, Africa – green, Europe – yellow, North America – blue). The sensitive isolate is denoted with a black arrow.

and the most distant, HAP_B12, all composed of Asian and North American isolates (Figure 3B). A similar topology was observed between the haplotype networks generated for *A. tenuissima* isolates. For both *CYP*51 and *CYP*61, the isolate FERA 648 was observed to branch off separately from the largest haplotype containing identical isolates (Figure 3C, Figure 3D). In the haplotype network for *CYP*51, only isolates FERA 1164 and FERA 24350 exhibited numerous mutations to form a distinct haplotype. In contrast, two distinct lineages had formed from the sensitive haplotype HAP_D2, with one consisting of haplotypes HAP_D3 and HAP_D4, and the other lineage comprised solely by the isolate FERA 1166 of HAP_D1 (Figure 3C).

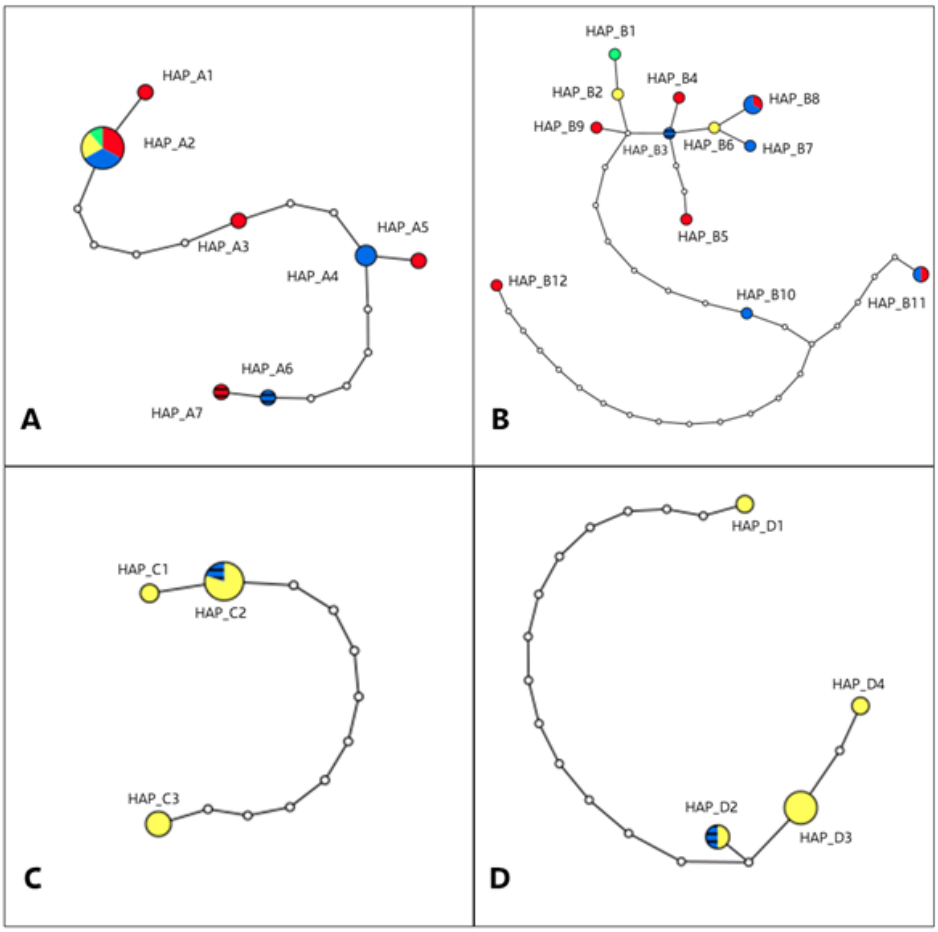

Figure 3. TCS statistical parsimony haplotype networks generated for 15 *CYP*51 **(A)** and *CYP*61 **(B)** sequences from *Alternaria alternata* (representing 4 geographic regions) and 8 *CYP*51 **(C)** and *CYP*61 **(D)** sequences from *A. tenuissima* (representing 2 geographic regions). Each color represents a different geographic region (Asia – red, Africa – green, Europe – yellow, North America – blue). The size of the circle indicates the relative frequency of sequences belonging to a particular haplotype (smallest circle – 1 isolate, largest circle – 9 isolates). Haplotypes marked with horizontal stripes indicate sequences which were determined to be sensitive to DMI fungicides. Smaller circles represent putative haplotypes, with the partitioning lines indicating the genetic distance between each haplotype.

Estimation of genetic clustering patterns and inference evolutionary parameters of populations of *A. alternata* and *A. tenuissima*. The various genetic diversity parameters were calculated across isolates of *A. alternata* and *A. tenuissima* based on *CYP*51, *CYP*61, and ITS regions. While 49 variable sites were observed in *A. alternata, only* 29 variable sites were observed in *A. tenuissima*. This indicates a greater number of polymorphic or parsimonious sites specific to the C*YP*51 and *CYP*61 gene regions present across *A. alternata* when compared to *A. tenuissima*. Results from DnaSP showed that 15 completely distinct haplotypes for the three gene regions (i.e., *CYP*51, *CYP*61, and ITS) were observed for all 15 *A. alternata* isolates. In contrast, only 6 haplotypes were observed for *A. tenuissima* with a haplotype diversity of 89.3%. A nucleotide diversity (π) of 0.00290 and Θ_w of 0.00359 was observed across isolates of *A. alternata* while a π of 0.002211 and Θ_w of 0.00261 across isolates of *A. tenuissima*. Based on the calculated Tajima's D values, fewer haplotypes were observed than the number of segregating sites. Thus, based on the identification of parsimonious sites, signatures of purifying positive selection were observed across the two species (Table 5).

Table 5. Genetic diversity parameters of isolates of *A. alternata* and *A. tenuissima* based on *CYP*51, *CYP*61, and ITS regions

Species	N[1]	VS[2]	π[3]	Hd[4]	Θ_w[5]	Tajima's D[6]
A. alternata	15	49	0.00290	1.000 (15)	0.00359	-0.82745
A. tenuissima	8	29	0.002211	0.893 (6)	0.00261	-0.79737

[1]Number of isolates; [2]Number of variable sites; [3]Nucleotide diversity; [4]Haplotype diversity and number of haplotypes (in parenthesis); [5]Watterson's estimator; [6]Tajima's D value.

DISCUSSION

*CYP*51 is a highly conserved protein that has a strong specificity, serving an essential and crucial function in the biosynthesis of ergosterol. It is involved in the conversion of 14α-demethylase which is inhibited when targeted by azole fungicides, thereby reducing growth due to the degradation of ergosterol. The accumulation of point mutations in the fungal gene was attributed to decreased sensitivity to DMI fungicidal action (Parker et al. 2014). Moreover, *ERG*5 is a sterol C-22 desaturase (*CYP*61) involved in the late steps of ergosterol biosynthesis. Antifungal azoles inhibit ergosterol biosynthesis by interfering with lanosterol 14α-demethylase. Thus, understanding the patterns and cause behind the mutations occurring in this gene region could provide a new perspective such as in the recommended use of those currently available in the market or when developing new products or formulations to help address azole resistance in *A. alternata* and *A. tenuissima*. Current methods which involve the temporal rotation in the use of different

types of fungicides, the regulation of fungicide concentration used, and the use of preventive over eradicative or curative applications are suggested to reduce the growing incidence of fungicide resistance (Rossi et al. 2021).

Based on initial surveys, nucleotide variation based on DnaSP analyses of identified parsimonious sites were abundant across multiple strains of both species when compared to the sensitive isolate. For *A. alternata*, the North American isolate obtained from sewage treatment (SRC1lrK2f) especially was found to contain numerous gaps of 10-20 base pairs in length when compared to isolates with similar nucleotide sequences, such as the Indian isolates from *Brassica juncea*. This may be due to prolonged exposure to high concentrations of fungicidal agents with a similar mode of action to DMI fungicides from environmental contamination (Zubrod et al. 2019). Avenot et al. (2016) describes cross-resistance present in *Alternaria* leaf blight in California pistachios against the three types of DMI fungicides highlighted in the findings of this study. The emergence of cross-resistance may be partially attributed to multi-target fungicides, which act as selection pressures, leading to the persistence of populations resistant to different classes of fungicides (Malandrakis et al. 2015; Yang et al. 2019). However, less variability was observed in the *CYP*61 sequence of SRC1lrK2f isolate despite the gene's prominent role in ergosterol biosynthesis. Variations in the abundance of mutations between *CYP*51 and *CYP*61 were shown to be due to their timing in fungal ergosterol biosynthesis, with *CYP*51 coding for the enzyme 14α-demethylase which acts early in the process and *CYP*61 coding for C-5 sterol desaturase which acts much later. Moreover, difference in sensitivity patterns in response to DMI fungicide exposure across the two genes may also be a possible reason for this occurrence. Based on the results of the survey, *CYP*61 showed a much higher variability than *CYP*51 across isolates of both species.

Results of phylogenetic analysis in both species show the occurrence of two distinctive clades in the analysis of *CYP*51 and a highly variable tree topology and branching pattern for *CYP*61. This would indicate similar mutation patterns present between the two species in the two most prominent genes affected by DMI fungicides. The frequency and recurrence of the point mutations observed in both species were considerable based on the estimation of genetic clustering patterns and these indicated the significance of these gene regions in the development of fungicide resistance by genetic variability. Signatures of positive selection were present in populations of *A. alternata* and *A. tenuissima* across a diverse scope of geographic locations and host species. This mechanism was shown to be more pronounced with *A. alternata* due to the number of variable sites observed in isolates. The shared haplotypes of *A. alternata* isolates indicate genetic clustering and

support the presence of selection pressures found in the two gene regions. Results from nucleotide and haplotype diversity estimation reinforce the significance of these gene regions in the susceptibility of fungal pathogens to DMI fungicides. Generally, environmental conditions such as temperature and topography are shown to increase the persistence of DMI fungicide resistance which was shown to be a quantitative evolutionary trait in *A. alternata* (He et al. 2019). However, the use of specific crop varieties to mitigate the development of fungicide resistance was shown to be insignificant. A previous study on spring barley powdery mildew caused by *Erysiphe graminis* showed that no significant differences were observed in the DMI sensitivity across cultivars of the crop (Brent et al. 1989). This suggests that host crop variety may not be a driving selection pressure for the development of DMI fungicide resistance. Meanwhile, the lower haplotype diversity based on estimation of genetic diversity parameters and haplotype analyses of *A. tenuissima* indicate the presence of a less stringent selection pressure driving the population structure of the fungal pathogen based on the genetic diversity across the two regions represented. Overall, these findings from the analysis of genetic clustering patterns based on the sensitivity profile, environmental exposures based on metadata, host species of origin, and geographic location across strains from both species provide a possible basis for the differences observed corresponding to identified haplotypes.

Results from the statistical analysis of the EC_{50} values of *A. alternata* tested with difenoconazole, tebuconazole, and propiconazole showed that the type of fungicide used would not affect the severity of resistance in the fungal pathogen. These findings would indicate a clear correlation between the accumulation of point mutations in *CYP*51 and *CYP*61 genes of *A. alternata* and *A. tenuissima*, with the latter forming a pattern unrelated to geographic location. Previous studies show that the selection against resistant mutants harmonizes the genetic difference of geographically distant populations accumulated by random drift (He et al. 2019). However, the lack of metadata on the DMI fungicide sensitivity profile of certain isolates included in the study hindered any further investigation on the association of the aforementioned factors. Inferences were made based on isolates clustering together, with the sensitive isolate also displaying a similar sensitivity profile while isolates that had accumulated a greater number of mutations would confer some level of resistance (Chen et al. 2014; He et al. 2019; Armitage et al. 2020).

The occurrence of selection based on the *CYP*51 gene is likely based on the patterns observed and the similarities in the mutation patterns generally found across the isolates analyzed. This pattern of DMI fungicide resistance was also clearly

observable in previous studies on the *CYP*51 gene regions of *Pyrenophora teres* f. sp. *teres* infecting barley plants and the wheat pathogen *Parastogonospora nodorum* (Mair et al. 2016; Pereira et al. 2021). The linearity of the observed evolutionary pattern further reinforces the presence of selection. For *CYP*61, the variability of the evolutionary patterns would indicate the occurrence of random selection with no distinctive specificity towards DMI exposure. However, the general clustering pattern observed across most of the isolates is highly indicative of an underlying mechanism, supporting the presence of a mutative response in *CYP*61, as well. Currently, there is an insufficient number of recent studies which have attempted to characterize the evolutionary patterns of *CYP*61 gene region despite its established contribution in DMI fungicide resistance development (Kelly et al. 1997; Lamb et al. 1999). Further analysis and testing on other factors associated would provide more insight on this mutative pattern.

In general, the patterns observed in the Asian and North American *A. alternata* isolates were relatively consistent across both gene regions investigated, with some degree of variation observed in the European and African isolates. As such, selection in *A. alternata* in these geographic regions has a high likelihood of occurring and persisting without proper intervention despite the relatively low risk of DMI fungicide resistance occurring. The two geographic regions investigated for *A. tenuissima*, Europe and North America, showed a generally consistent pattern and a relative likelihood of selection events occurring in European isolates. This is due to the identical nucleotide sequences observed in the *CYP*51 and *CYP*61 gene regions analyzed. Therefore, mitigation methods should be improved to prevent the development of fungicide resistance in these geographic regions. Such methods would include the spatiotemporal rotation of fungicide use to generate diversifying selection across affected populations (He et al. 2019). Moreover, effective global mitigation schemes to prevent migration events associated with fungicide resistance development may be implemented with the globalization of agricultural production (Zhang et al. 2019; Zhang et al. 2020).

From the findings of the study, genetic diversity with distinct patterns based on DMI fungicide gene targets *CYP*51 and *CYP*61 in *A. alternata* and *A. tenuissima* was observed as illustrated through phylogenetic analysis with well supported clades. The nucleotide sequences of the gene regions of each species showed an abundance of point mutations, many of which bore similarities across several isolates. Clustering patterns around sensitive isolates for the consensus trees were observed based on the geographic regions of origin though no distinctive trends had formed based on host species of origin. The initially inferred genetic

clustering patterns based on the BLAST identity and point mutations patterns of nucleotide sequences were further supported by the diversity metrices estimated. The evolutionary pattern observed reinforced the presence of selection pressures based on DMI fungicide exposure as exhibited in the gene target regions. These results, along with the estimated genetic diversity parameters, showed indications for positive selection occurring across alleles favoring the capability of the fungal populations to overcome deleterious effects of DMI fungicides and subsequently persist in the field.

For a future direction of the study, the investigation of cross-resistance in fungal pathogen species in response to exposure to various types of fungicides can be done. Cross-resistance to DMI fungicides may occur due to its high specificity to its specific target (Malandrakis et al. 2015; Avenot et al. 2016; Yang et al. 2019). Variations in gene expression, which have been previously shown to induce resistance by altering the sensitivity of enzymatic targets to DMI fungicidal action can be further explored (Parker et al. 2014; Zhang et al. 2019). The analysis of temporal and host specific patterns can also be done to trace the evolutionary history gene *CYP*51 and other genes involved in the biosynthesis of ergosterol. The timespan of evolution is an essential factor shaping the impact of selection pressures shaping populations of fungal pathogens. This could be further integrated with the observed phylogeographic patterns to consolidate a dynamic prevention scheme which accounts for the different factors involved in fungicide resistance development. Additionally, to supplement and confirm *in silico* findings and theories, in vitro and *in enviro* testing on live isolates associated with their hosts can be done. Increasing the number of *A. Alternaria* and *A. tenuissima* sequence datasets and expanding the geographic region representation of the phylogeographic analysis would help to improve robustness of the patterns of fungicide resistance development observed. The implementation of fine-scale population genetic analyses utilizing this approach can help to elucidate the projected patterns observed in the current study. A similar approach to survey the widespread prevalence can be done to analyze the significance of the EC_{50} values and sensitivity patterns observed in the isolates obtained. From these findings, dynamic and effective mitigation methods concurring with molecular and phenotypic evidence of fungicide resistance development can be formed and utilized in the agricultural industry.

REFERENCES

Ali M, Ahmed M, Ramadan M, Ibrahim S. 2019. Effect of fungicides, antioxidants and their mixtures on mycelial growth of some fungi. Middle East J Appl Sci. 08(02):647–655.

Amrate P, Nehru J, Vishwavidyalaya K, Sharma JR, Singh C. 2013. In vitro evaluation of fungicides, plant extracts and oils against Alternaria alternata (Fr.) keissler causing leaf spot of Aloe barbadensis (Miller). Asian J Microbiol Biotechnol Environ Sci. 15(3):609–613.

Armitage AD, Cockerton HM, Sreenivasaprasad S, Woodhall J, Lane CR, Harrison RJ, Clarkson JP. 2020. Genomics Evolutionary History and Diagnostics of the Alternaria alternata Species Group Including Apple and Asian Pear Pathotypes. Front Microbiol. 10. doi:10.3389/fmicb.2019.03124.

Arnaoudova E, Haws DC, Huggins P, Jaromczyk JW, Moore N, Schardl CL, Yoshida R. 2010. Statistical phylogenetic tree analysis using differences of means. Front Neurosci. 4(AUG). doi:10.3389/fnins.2010.00047.

Avenot HF, Solorio C, Morgan DP, Michailides TJ. 2016. Sensitivity and cross-resistance patterns to demethylation-inhibiting fungicides in California populations of Alternaria alternata pathogenic on pistachio. Crop Prot. 88:72–78. doi:10.1016/j.cropro.2016.05.012.

Bihon W, Cloete M, Gerrano AS, Oelofse D, Adebola P. 2016. Draft genome sequence of Alternaria alternata isolated from onion leaves in South Africa. Genome Announc. 4(5). doi:10.1128/genomeA.01022-16.

Brent KJ, Carter GA, Hollomon DW, Hunter T, Locke T, Proven M. 1989. Factors affecting build-up of fungicide resistance in powdery mildew in spring barley. Neth J Plant Pathol. 95:31–41. doi:10.1007/BF01974282.

Chen W, Lee MK, Jefcoate C, Kim SC, Chen F, Yu JH. 2014. Fungal cytochrome P450 monooxygenases: Their distribution, structure, functions, family expansion, and evolutionary origin. Genome Biol Evol. 6(7):1620–1634. doi:10.1093/gbe/evu132.

Chong P, Essoh JN, Arango Isaza RE, Keizer P, Stergiopoulos I, Seidl MF, Guzman M, Sandoval J, Verweij PE, Scalliet G, et al. 2021. A world-wide analysis of reduced sensitivity to DMI fungicides in the banana pathogen Pseudocercospora fijiensis. Pest Manag Sci. 77(7):3273–3288. doi:10.1002/ps.6372.

Dang HX, Pryor B, Peever T, Lawrence CB. 2015. The Alternaria genomes database: A comprehensive resource for a fungal genus comprised of saprophytes, plant pathogens, and allergenic species. BMC Genomics. 16(1). doi:10.1186/s12864-015-1430-7.

Deising H, Reimann S, Pascholati S. 2008. Mechanisms and Significance of Fungicide Resistance. Braz J Microbiol. 39:286–295. doi:10.1590/S1517-838220080002000017.

dos Santos A, Cabezas M, Tavares A, Xavier R, Branco M. 2016. TcsBU: A tool to extend TCS network layout and visualization. Bioinform. 32(4):627–628. doi:10.1093/bioinformatics/btv636.Fu Y, Mei X, Han G, Li H. 2017. Sensitivity assay of Alternaria alternata tangerine pathotype from China to tebuconazole and difenoconazole using resazurin-based microtiter. Chin J Pestic Sci. 19(5):543–549. doi:10.16801/j.issn.1008-7303.2017.0072.

Gai Y, Liu B, Ma H, Li L, Chen X, Moenga S, Riely B, Fayyaz A, Wang M, Li H. 2019. The methionine biosynthesis regulator AaMetR contributes to oxidative stress tolerance and virulence in Alternaria alternata. Microbiol Res. 219:94–109. doi:10.1016/j.micres.2018.11.007.

Gai Y, Ma H, Chen Y, Li L, Cao Y, Wang M, Sun X, Jiao C, Riely BK, Li H. 2021. Chromosome-scale genome sequence of Alternaria alternata causing alternaria brown spot of citrus. Mol Plant Microbe Interact. 34(7). doi:10.1094/MPMI-10-20-0278-SC.

Gebru ST, Gangiredla J, Tournas VH, Tartera C, Mammel MK. 2020. Draft Genome Sequences of Alternaria Strains Isolated from Grapes and Apples. Microbiol Resour Announc. 9(14). doi:10.1128/MRA.

Hall BG. 2013. Building phylogenetic trees from molecular data with MEGA. Mol Biol Evol. 30(5):1229–1235. doi:10.1093/molbev/mst012.

He MH, Wang YP, Jiao Wu E, Shen LL, Yang LN, Wang T, Shang LP, Zhu W, Zhan J. 2019. Constraining Evolution of Alternaria alternata Resistance to a Demethylation Inhibitor (DMI) Fungicide Difenoconazole. Front Microbiol. 10. doi:10.3389/fmicb.2019.01609.

Kelly SL, Lamb DC, Baldwin BC, Corran AJ, Kelly DE. 1997. Characterization of Saccharomyces cerevisiae CYP61, Sterol 22-Desaturase, and Inhibition by Azole Antifungal Agents*. J Biol Chem. 272(15):9986-9988. doi:10.1074/jbc.272.15.9986.

Kumar S, Stecher G, Li M, Knyaz C, Tamura K. 2018. MEGA X: Molecular evolutionary genetics analysis across computing platforms. Mol Biol Evol. 35(6):1547–1549. doi:10.1093/molbev/msy096.

Lamb DC, Maspahy S, Kelly DE, Manning NJ, Geber A, Bennett JE, Kelly SL. 1999. Purification, Reconstitution, and Inhibition of Cytochrome P-450 Sterol 22-Desaturase from the Pathogenic Fungus Candida glabrata. Antimicrob Agents Chemother. 43(7):1725–1728. doi:10.1128/AAC.43.7.1725.

Loto I, Gutiérrez MS, Barahona S, Sepúlveda D, Martínez-Moya P, Baeza M, Cifuentes V, Alcaíno J. 2012. Enhancement of carotenoid production by disrupting the C22-sterol desaturase gene (CYP61) in Xanthophyllomyces dendrorhous. BMC Microbiol. 12. doi:10.1186/1471-2180-12-235.

Mair WJ, Deng W, Mullins JGL, West S, Wang P, Besharat N, Ellwood SR, Oliver RP, Lopez-Ruiz FJ. 2016. Demethylase inhibitor fungicide resistance in *Pyrenophora teres f. sp. teres* associated with target site modification and inducible overexpression of Cyp51. Front Microbiol. 7(AUG). doi:10.3389/fmicb.2016.01279.

Malandrakis AA, Apostolidou ZA, Markoglou A, Flouri F. 2015. Fitness and cross-resistance of Alternaria alternata field isolates with specific or multiple resistance to single site inhibitors and mancozeb. Eur J Plant Pathol. 142(3):489–499. doi:10.1007/s10658-015-0628-5.

Mesny F, Miyauchi S, Thiergart T, Pickel B, Atanasova L, Karlsson M, Hüttel B, Barry KW, Haridas S, Chen C, et al. 2021. Genetic determinants of endophytism in the Arabidopsis root mycobiome. Nat Commun. 12(1). doi:10.1038/s41467-021-27479-y.

Nguyen HDT, Lewis CT, Lévesque CA, Gräfenhan T. 2016. Draft genome sequence of Alternaria alternata ATCC 34957. Genome Announc. 4(1). doi:10.1128/genomeA.01554-15.

Ostertagova E, Ostertag O, Ostertagová E. 2013. Methodology and Application of One-way ANOVA. Am J Mech Eng. 1(7):256–261. doi:10.12691/ajme-1-7-21.

Ozkilinc H, Kurt S. 2017. Screening Fungicide Resistance of Alternaria Pathogens Causing Alternaria Blight of Pistachio in Turkey. Yuzuncu Yil University J Agric Sci. 27(4):543–549. doi:10.29133/yyutbd.339081.

Park SY, Jeon J, Kim JA, Jeon MJ, Jeong MH, Kim Y, Lee Y, Chung H, Lee YH, Kim S. 2020. Draft Genome Sequence of Alternaria alternata JS-1623, a Fungal Endophyte of Abies koreana. Mycobiology. 48(3):240–244. doi:10.1080/12298093.2020.1756134.

Parker JE, Warrilow AGS, Price CL, Mullins JGL, Kelly DE, Kelly SL. 2014. Resistance to antifungals that target CYP51. J Chem Biol. 7(4):143–161. doi:10.1007/s12154-014-0121-1.

Pastor FJ, Guarro J. 2008. Alternaria infections: Laboratory diagnosis and relevant clinical features. Clin Microbiol Infect. 14(8):734–746. doi:10.1111/j.1469-0691.2008.02024.x.

Patriarca A, Fernández Pinto V. 2018. Alternaria. Reference Module in Food Science.:1–8. doi:10.1016/B978-0-08-100596-5.22572-9.

Pereira D, McDonald BA, Croll D. 2021. The genetic architecture of emerging fungicide resistance in populations of a global wheat pathogen. Genome Biol Evol. 12(12):2231–2244. doi:10.1093/GBE/EVAA203.

Rajarammohan S, Paritosh K, Pental D, Kaur J. 2019. Comparative genomics of Alternaria species provides insights into the pathogenic lifestyle of Alternaria brassicae - A pathogen of the Brassicaceae family. BMC Genomics. 20(1). doi:10.1186/s12864-019-6414-6.

Rosenzweig N, Hanson LE, Mambetova S, Jiang QW, Guza C, Stewart J, Somohano P. 2019. Fungicide sensitivity monitoring of Alternaria spp. causing leaf spot of sugarbeet (Beta vulgaris) in the Upper Great Lakes. Plant Dis. 103(9):2263–2270. doi:10.1094/PDIS-12-18-2282-RE.

Rossi V, Caffi T, Legler SE, Fedele G. 2021. A method for scoring the risk of fungicide resistance in vineyards. Crop Prot. 143. doi:10.1016/j.cropro.2020.105477.

Rozas J, Ferrer-Mata A, Sanchez-DelBarrio JC, Guirao-Rico S, Librado P, Ramos-Onsins SE, Sanchez-Gracia A. 2017. DnaSP 6: DNA sequence polymorphism analysis of large data sets. Mol Biol Evol. 34(12):3299–3302. doi:10.1093/molbev/msx248.

Schoch CL, Crous PW, Groenewald JZ, Boehm EWA, Burgess TI, de Gruyter J, de Hoog GS, Dixon LJ, Grube M, Gueidan C, et al. 2009. A class-wide phylogenetic assessment of Dothideomycetes. Stud Mycol. 64:1–15. doi:10.3114/sim.2009.64.01.

Shalini K, Kumar N, Drabu S, Sharma PK. 2011. Advances in synthetic approach to and antifungal activity of triazoles. Beilstein J Org Chem. 7:668–677. doi:10.3762/bjoc.7.79.

Snell Q, Posada D, Crandall KA. 2002. TCS: Estimating Gene Genealogies. Proceedings 16th International Parallel and Distributed Processing Symposium. 7. doi: 10.1109/IPDPS.2002.1016585.

Swofford, D.L., 2003. PAUP* ver 4.0. b10. Phylogenetic Analysis Using Parsimony and Other Methods. Sunderland, MA: Sinauer Associates, Sunderland.

Tamang P, Richards JK, Alhashal A, Sharma Poudel R, Horsley RD, Friesen TL, Brueggeman RS. 2019. Mapping of barley susceptibility/resistance QTL against spot form net blotch caused by Pyrenophora teres f. maculata using RIL populations. Theor Appl Genet. doi:10.1007/s00122-019-03328-x.

Wu JJ, Wu PC, Yago JI, Chung KR. 2023. The Regulatory Hub of Siderophore Biosynthesis in the Phytopathogenic Fungus Alternaria alternata. J Fungi. 9(4). doi:10.3390/jof9040427.

Yang LN, He MH, Ouyang HB, Zhu W, Pan ZC, Sui QJ, Shang LP, Zhan J. 2019. Cross-resistance of the pathogenic fungus Alternaria alternata to fungicides with different modes of action. BMC Microbiol. 19(1). doi:10.1186/s12866-019-1574-8.

Zeiner CA, Purvine SO, Zink EM, Paša-Tolić L, Chaput DL, Haridas S, Wu S, LaButti K, Grigoriev IV., Henrissat B, et al. 2016. Comparative analysis of secretome profiles of manganese(II)-oxidizing Ascomycete fungi. PLoS One. 11(7). doi:10.1371/journal.pone.0157844.

Zhang J, Li L, Lv Q, Yan L, Wang Y, Jiang Y. 2019. The fungal CYP51s: Their functions, structures, related drug resistance, and inhibitors. Front Microbiol. 10. doi:10.3389/fmicb.2019.00691.

Zhang Y, Zhou Q, Tian P, Li Y, Duan G, Li D, Zhan J, Chen F. 2020. Induced expression of CYP51 associated with difenoconazole resistance in the pathogenic Alternaria sect. on potato in China. Pest Manag Sci. 76(5):1751–1760. doi:10.1002/ps.5699.

Zubrod JP, Bundschuh M, Arts G, Brühl CA, Imfeld G, Knäbel A, Payraudeau S, Rasmussen JJ, Rohr J, Scharmüller A, et al. 2019. Fungicides: An Overlooked Pesticide Class? Environ Sci Technol. 53(7):3347–3365. doi:10.1021/acs.est.8b04392.

———

Robbi Miguel G. Falcon <rgfalcon@up.edu.ph> is a BS Biology graduate from the Institute of Biology, University of the Philippines Diliman. Currently, he is an MD-PhD Student in Molecular Medicine at the College of Medicine, University of the Philippines Manila. His research interests include medical mycology, immunology, and phylogenetics.

Leilani S. Dacones is an Assistant Professor of Mycology at the Institute of Biology in the University of the Philippines Diliman. Her current research focuses on determining the underlying genetic basis of host specialization, fungicide resistance, and the reproductive biology of plant pathogenic fungi affecting economically important crops.